

# Operator dynamics in $k$ -Markov random circuits

Unnati Akhouri,<sup>1,2</sup> Pei-Jun Huang,<sup>3</sup> Elliott Rose,<sup>1,2</sup> and Sarah Shandera<sup>1,4,2,\*</sup>

<sup>1</sup>*Institute for Gravitation and the Cosmos, The Pennsylvania State University, University Park, PA 16802, USA*

<sup>2</sup>*Department of Physics, The Pennsylvania State University, University Park, PA 16802, USA.*

<sup>3</sup>*Department of Physics, Brown University, Providence, RI 02912, USA*

<sup>4</sup>*Center for the Theory of Emergent Quantum Matter,*

*The Pennsylvania State University, University Park, PA 16802, USA*

(Dated: March 20, 2026)

We demonstrate that  $k$ -Markov sequences of unitary gates provide low-cost handles to manipulate the rate and structure of information spreading compared to traditional random, 0-Markov, circuits. For SWAP gates and brickwork circuits, we use graph cover time to demonstrate how  $k$ -Markov processes can be used to control operator transport. With SWAP gates and the set of Clifford gates that can change operator weight, we show how  $k$ -Markov sequences can be used to manipulate scrambling time and generate novel structures of spatial-temporal correlations across a qubit network. We show that  $k$ -Markov circuits constructed from PSWAP gates at fixed angle are equivalent to standard brickwork circuits with PSWAP angle drawn from non-uniform distributions generated by the  $k$ -Markov process. In those circuits, the time evolution of the average Hamming weight and the space-time correlation structure after equilibrium again vary significantly from the 0-Markov case, depending on the transition probabilities of the process.

Understanding and controlling the dynamics of quantum correlations is a rich and active area of study. In particular, in large, many-body systems it is interesting to understand the classes of dynamics under which initially localized properties of a state remain localized, in contrast to those where local information becomes delocalized in correlations among many degrees of freedom. A large body of literature studies these questions in the context of quantum circuits, often with the evolution at each layer chosen at random from some specified set of operations that may include unitary gates [1, 2], local measurements [3–5], and dissipation [6–8].

In this paper, we show how temporal correlations in a stochastic prescription for the unitary gates applied at each circuit layer can affect information dynamics. For circuits over a network of  $N$  qubits, consider a fixed set of unitaries that may act on the network, each constructed from a tensor product of  $p$ -local unitaries,  $p \leq N$ . Labeling each  $N$ -qubit unitary by a letter ( $A, B, \dots$ ) defines an alphabet from which a variety of stochastic sequences can be built, where the probability of a letter depends on  $k$  previous letters (the context). For  $k > 1$ , the sequences are  $k$ -Markov, often also called non-Markovian with context  $k$  [9]. In contrast, most studies of random circuits to date assume  $k = 0$ , or introduce temporal structure through measurement and feedback [10–12]. Here we show that  $k$ -Markov sequences provide operationally inexpensive dials to (statistically) control information dynamics without requiring mid-circuit disturbance of the state or real-time adjustment of the algorithm.

*Setting up the circuits* - We consider an alphabet of two letters ( $\mathbf{A}$ ,  $\mathbf{B}$ ), each defined by a particular choice of  $N$ -qubit unitary dynamics built from 2-local unitaries applied to nearest neighbor qubits in a 1-dimensional, closed chain. For simplicity, we assume  $N$  is even. From

$\mathbf{A}$  and  $\mathbf{B}$  we construct circuits using gate sequences determined by a  $k$ -Markov process. For example, 1-Markov sequences are defined by two transition probabilities. These specify the probability that the next letter in the sequence is  $\mathbf{A}$ , conditioned on the previous letter being either  $\mathbf{A}$ ,  $p(\mathbf{A}|\mathbf{A})$  or  $\mathbf{B}$ ,  $p(\mathbf{A}|\mathbf{B})$ . Similarly, a 2-Markov rule is specified by four probabilities,  $p(\mathbf{A}|\mathbf{AA})$ ,  $p(\mathbf{A}|\mathbf{AB})$ ,  $p(\mathbf{A}|\mathbf{BA})$ ,  $p(\mathbf{A}|\mathbf{BB})$ . (Of course, it is possible to choose probabilities at order  $k$  such that the rule is actually lower order Markov. We exclude those cases from results shown at order  $k$ .)

*Characterizing information dynamics* - To characterize the dynamics produced by the  $k$ -Markov gate sequences, we examine properties of  $\mathcal{O}(\ell) = U_\ell^\dagger \mathcal{O}(0) U_\ell$ , where  $U_\ell$  is the cumulative unitary evolution of the circuit through layer  $\ell$  and we take  $\mathcal{O}(0)$  to be an operator with a non-identity component on only a single site. We will use the Pauli words,  $\{\mathcal{P}_\alpha\}$ , as the basis for operators and write  $\mathcal{O}(\ell) = U_\ell^\dagger \mathcal{O}(0) U_\ell = \sum_\alpha c_\alpha(\ell) \mathcal{P}_\alpha$ . The (Hamming) weight of each word is the number of non-identity components. While in general there are  $4^N$  words, different choices of the allowed unitaries in the circuit and the initial operator can restrict the number of reachable Pauli strings,  $R_{\text{reachable}}(\mathcal{O}(0), \{U\}) < 4^N$ , that can ever have non-zero weight in the evolved operator.

*SWAP gates and cover time* - We first demonstrate the relationship between  $k$ -Markov sequences and operator spreading in a simple case of only SWAP gates. With this dynamics, an initial single-site operator (we use  $\sigma_z$ ) will simply move across the qubit network with time. The difference between dynamics can be quantified with cover time,  $t_c$ , which is the smallest number of circuit layers before every site has hosted  $\sigma_z$  at least once. Consider the two-letter alphabet where the  $N$ -qubit unitaries are  $\mathbf{A}_{\text{SWAP}}$  and  $\mathbf{B}_{\text{SWAP}}$  correspond to pairing each qubit to

its left or right neighbor with a SWAP gate. Then, in the unbiased 0-Markov model, each layer of the circuit is chosen independently and with equal probability. The dynamics is an unbiased random walk on a one-dimensional cycle graph and  $\langle t_c \rangle = \frac{N(N-1)}{2}$  [13]. For simplicity, fix  $P(A) = P(B)$ . Then in each  $k$ -Markov model all probabilities will be symmetric under exchange of  $\mathbf{A}$  and  $\mathbf{B}$ , but the mean and distribution of cover times will in general be quite different from those of the unbiased random walk.

The shortest cover time in the SWAP gate case would be given by the (deterministic) sequence  $\mathbf{A}_{\text{SWAP}}\mathbf{B}_{\text{SWAP}}\mathbf{A}_{\text{SWAP}}\mathbf{B}_{\text{SWAP}}\dots$  of length  $N$ . On the other hand, a sequence of only  $\mathbf{A}_{\text{SWAP}}$  or only  $\mathbf{B}_{\text{SWAP}}$  would localize the operator forever to just two sites. So,  $k$ -Markov processes will generate slower cover times when they bias the walk away from this optimal sequence. For 1-Markov processes, the cover time will be correlated with the probability of optimal sequences ( $\mathbf{A}_{\text{SWAP}}\mathbf{B}_{\text{SWAP}}$  or  $\mathbf{B}_{\text{SWAP}}\mathbf{A}_{\text{SWAP}}$ ), which is governed entirely by the probability to switch letters,  $P_{\text{switch}} = P(A|B) = P(B|A)$ . Switching probabilities above (below) 0.5 will generate mean cover times that are shorter (longer) than that of the random walk. As  $k$  is increased, the longer context allows choices that can help enforce the optimal trajectory.

The upper panel of Figure 1 shows the mean cover time (and  $\pm 1\sigma$  spread over 500 trials) of several  $k$ -Markov rules at varying network size,  $N$ . All rules share a common  $P(\text{switch}) = 0.95$ , which significantly reduces cover time compared to the 0-Markov circuit. The dynamics of each process can be concisely described by its diffusion coefficient,  $D$ , which can be analytically computed from the transition probabilities in some cases [14], or numerically computed by fitting the large- $N$  limit of each sequence ( $t_c = N^2/4D$ ). For system size approximately  $N < D$ , the processes can maintain nearly ballistic motion of the operator, while for larger systems the errors from the optimal gate sequence build up sufficiently that the cover times again scale as  $N^2$ . Of course, different choices of the transition probabilities can lead to arbitrarily long cover times.

*Operator growth with Clifford gates* - While in the previous example the operator weight was always 1, most unitary processes can change the weight, spreading the operator over multiple sites so that  $w(t)$  grows. To consider what kind of dials the  $k$ -Markov processes can provide in that case, we next consider alphabets built of the SWAP gate (weight preserving) and the set of Clifford gates that can change operator weight. Of the 720 Clifford gates (ignoring those that only change single-site phases), 648 gates cause transitions between at least one single-site operator and a two-site operator (increasing or decreasing the weight). A standard brickwork circuit with gates drawn at random from this set will increase operator weight faster thanks to the removal of the weight-

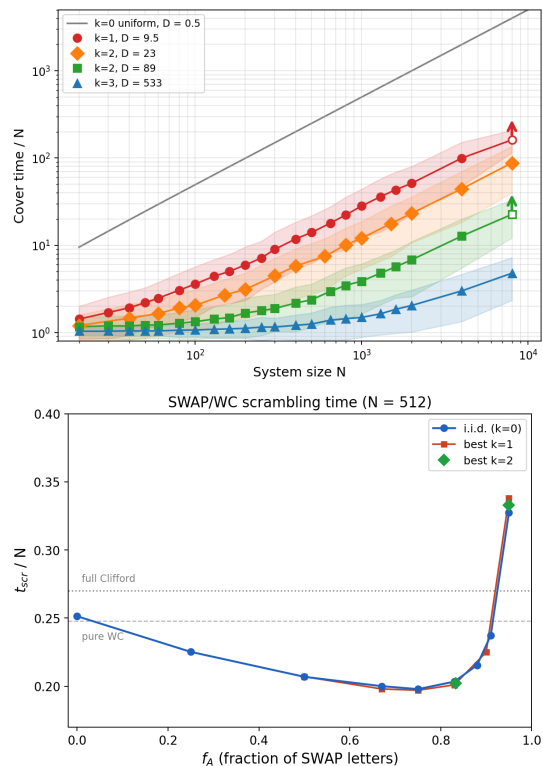


FIG. 1: **Top:** Mean cover times over system size,  $\langle t_c \rangle / N$  for  $k$ -Markov SWAP circuits as a function of  $N$ , for several different rules. The effective diffusion constant,  $D$ , is a function of the transition probabilities and controls the shift from nearly ballistic operator motion for smaller systems to diffusive transport in larger systems. Open symbols are used for cases where less than 90% of runs reached full coverage before the limit  $200N$  steps. For the  $k = 1$  example, only 54% finished, while the  $k = 2$  example had 87% finish. For those cases the position of the point is a lower bound on the mean cover time, biased low. Shaded regions show the  $1\sigma$  variation over 500 trials. **Bottom:** Scrambling times in Clifford weight-changing circuits, as a function of the fraction of SWAP single-layer ( $\mathbf{A}_{\text{SWAP}}$ ), for  $k = 0$  rules and the shortest times found for  $k = 1$  and  $k = 2$ , all for  $N = 512$ .

conserving gates. However, the inclusion of SWAP gate layers can further accelerate growth by increasing the probability that the leading edge of non-trivial operator support moves outward. Consider fixed brickwork geometry, again an alphabet with two letters,  $\mathbf{A}_{\text{SWAP}}$  and  $\mathbf{B}_{\text{WC}}$ . Now  $\mathbf{A}_{\text{SWAP}}$  applies SWAP gates to each qubit pair, while  $\mathbf{B}_{\text{WC}}$  chooses a (Haar) random gate from the weight-changing (WC) set. Different dynamics can be achieved by choosing  $\mathbf{A}_{\text{SWAP}}$  and  $\mathbf{B}_{\text{WC}}$  to act on a consecutive pair of layers of brickwork (even and odd), or to break parity and act on a single layer (even or odd).

To compare operator growth between models, we use

the scrambling time,  $t_{\text{scr}}$ , defined as the first layer for which the operator weight satisfies  $w(\ell) \geq \frac{N}{2}$ . For  $k = 0$  circuits, the scrambling time depends on the fraction of  $\mathbf{A}_{\text{SWAP}}$  gates,  $f_A$ . At  $k = 1, 2$ , we find that the scrambling time can only increase when  $\mathbf{B}_{\text{WC}}$ ,  $\mathbf{A}_{\text{SWAP}}$  each act on the even and odd bricklayers. When each letter is defined to act on only one layer (odd or even), only very small decreases in  $\langle t_{\text{scr}} \rangle$  can be achieved, where the optimal  $f_A$  increases with  $N$ . The bottom panel of Figure 1 shows how  $t_{\text{scr}}$  scales with the fraction of single-layer  $\mathbf{A}_{\text{SWAP}}$  letters,  $f_A$ , for  $k = 0$  processes and  $N = 512$ . It also shows that the shortest  $t_{\text{scr}}$  achieved with single-layer letters in scans over probabilities at fixed  $f_A$  lie very close to the  $k = 0$  line.

While different  $k$ -Markov sequences may give the same mean scrambling time, they generate distinguishable spatial-temporal correlations that are strongest before  $\langle t_{\text{scr}} \rangle$ , but also persist at very late times. Figure 2 shows several visualizations of the occupation at each site  $i$ :  $n_i = 1$  if the site hosts a non-identity operator, and is 0 otherwise. The Figure shows a heatmap of occupation for 512 qubits (black is the identity operator,  $n = 0$ ) in panel (a), as well as several examples of the correlation function

$$C(\Delta x, \Delta t) = \frac{\langle n_i(x, t) n_i(x + \Delta x, t + \Delta t) \rangle - \langle n_i(x, t) \rangle^2}{(\langle n_i(x, t) \rangle - \langle n_i(x, t) \rangle)^2} \quad (1)$$

where the average is over five realizations of each rule, all sites, and approximately 1000 late-time steps (at  $t > 2t_{\text{scr}}$ ). Panel (b) shows the late-time correlation function ( $t \gg t_{\text{scr}}$ ) for  $k = 0$ ,  $f_A = 0.83$  and double-layer letters. The lower two panels show the difference between the correlation function for  $k = 1$ ,  $f_A = 0.83$ ,  $\lambda = 1 - \frac{P(A|B)}{1-f_A}$  and the  $k = 0$  correlation, for both single- and double-layer letters. Even at  $k = 0$ , structure in  $C$  from the SWAP gate transport is visible, but higher  $k$  generates additional correlation.

*PSWAP circuits* - Finally, we consider a class of circuits where operator weight and complexity can both grow, constructed the alphabet from two-qubit partial swaps (PSWAPs) with fixed angle  $\theta$ . We restrict PSWAP to act in the charge 1 sector only, since this reduces the number of Pauli strings reachable from  $\sigma_z$  to  $2N^2$  (for a 1-dimensional ring of qubits) and allows for a simpler analytic understanding of the effects. While Clifford circuits map Pauli strings to Pauli strings and thus significantly restrict the dynamics, PSWAP circuits map a Pauli string into a linear combination of Pauli strings. One measure of how the operator spreads is the time-evolution of its average Hamming weight,  $w_{\text{ave}}(\ell) = \frac{1}{C(\ell)} \sum_{\alpha} |c_{\alpha}(\ell)|^2 w_{\alpha}$ .

As in the SWAP operator example, we take  $\mathbf{A}_{\text{PSWAP}}$  to be one of the two bricklayer couplings and  $\mathbf{B}_{\text{PSWAP}}$  to be the other. These PSWAP circuits can be directly connected to the large literature on random circuits that uses a brickwork pattern, drawing independent unitaries

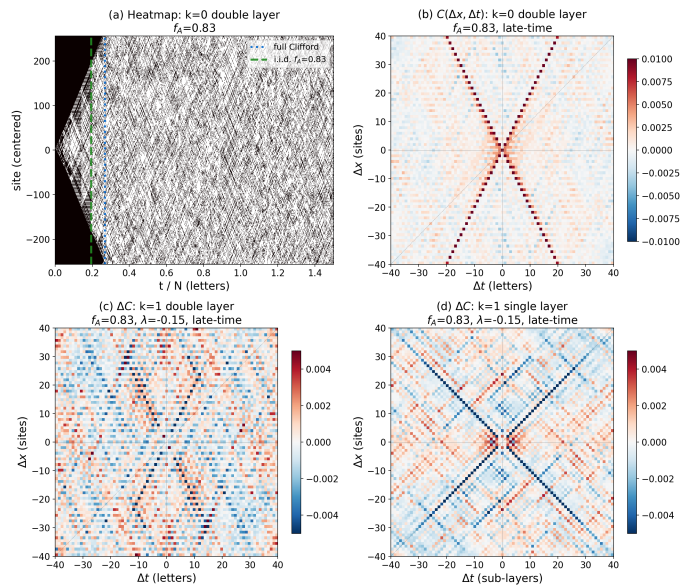


FIG. 2: Panel (a) operator structure for one realization of a  $k = 0$  rule. The signatures of the SWAP gate transport are most visible before  $t_{\text{scr}}$ , but partially retained even at very late times. (b) The late-time ( $t \gg t_{\text{scr}}$ ) correlation structure  $C(\Delta x, \Delta t)$  averages over sites and 5 realizations. (c) and (d) The difference between double-layer and single-layer  $k = 1$  late-time correlations and those of  $k = 0$  at matched  $f_A = 0.83$ .

from set for each layer [2]. This is because each string of  $m$  consecutive layers of  $\mathbf{A}_{\text{PSWAP}}$  can be collapsed into a single  $\mathbf{A}$ -type layer, where each 2-qubit unitary satisfies  $(U_{i,i+1}(\theta))^{m} = U_{i,i+1}(R_A \theta)$ , and similarly for the next set of  $\mathbf{B}$  layers. The circuits now have standard brickwork geometry, but where the evolution at compressed layer  $\ell$  is given by

$$U(\ell) = \prod_j U(R_{A,\ell} \theta)_{2j-1,2j} \prod_j U(R_{B,\ell} \theta)_{2j,2j+1}. \quad (2)$$

These are brickwork circuits with each  $R_{A,\ell}, R_{B,\ell}$  drawn from distributions inherited from the  $k$ -Markov rule. Unbiased, 0-Markov circuits give probability distribution  $P(R_A) = P(R_B) = 2^{-R_{A,B}}$ , while Bernoulli 0-Markov gives correlated geometric distributions. The statistics for  $m, n$  in other cases are those of the same-letter run lengths of the  $k$ -Markov sequence [15]. At  $k = 1$ , the sequences generate distributions over a discrete set of PSWAP angles that are independently geometric for odd and even layers, with mean given by  $P(A|B)$  and  $P(B|A)$ . At  $k = 2$ , the distributions for angle are no longer geometric, since the probability to enter either single-letter run need not be simply related to the probability of staying in the run. At  $k \geq 3$ , the distributions for temporally separated single-letter run lengths start to be correlated, as long as typical run lengths are shorter

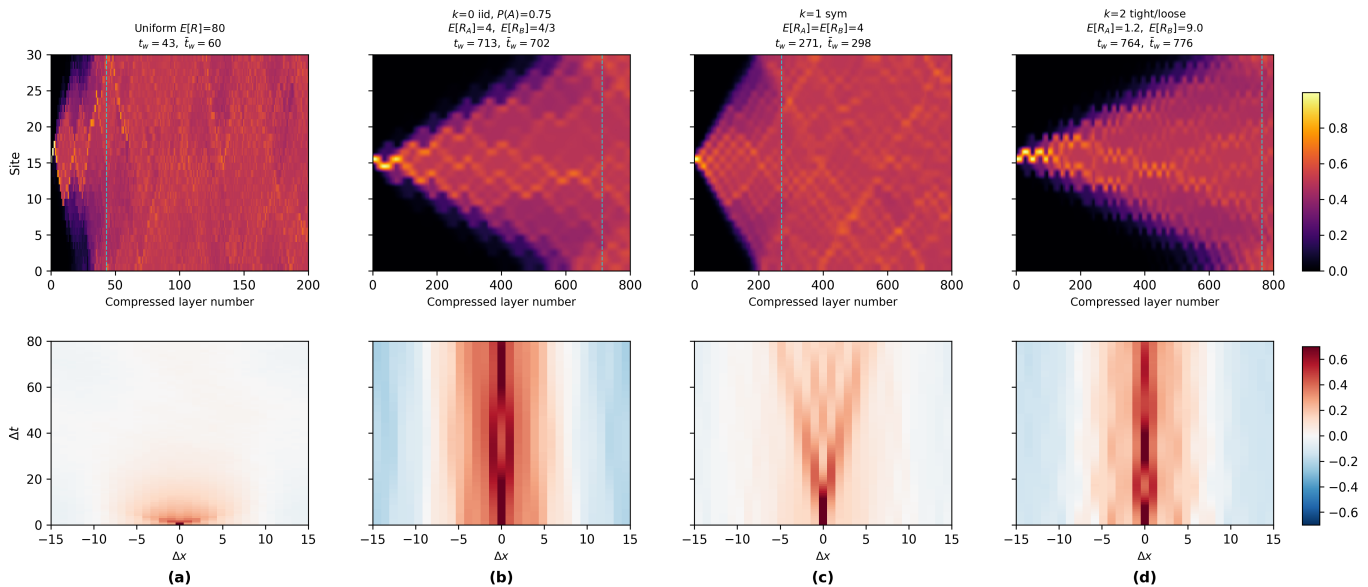


FIG. 3: Heatmaps (upper panels, one realization) and late-time spatial-temporal correlation structure (lower panels, averaged over five realizations, all sites, and about 1000 layers well after the network weight has equilibrated past the threshold) for a 30-qubit network, under four different rules for generating run-length distributions as follows **(a)** Uniformly distributed, with average length  $E[R_A] = E[R_B] = 80$ ; **(b)** Generated by a  $k = 0$  process for the  $A, B$  alphabet, where  $P(A) = 0.75$  sets the geometric distributions  $E[R_A] = 4$ ,  $E[R_B] = 4/3$ ; **(c)** Generated by a  $k = 1$  process where the geometric distributions for  $R_A, R_B$  are chosen to be the same; **(d)** Generated by a  $k = 2$  process with different expectation values for  $A$  and  $B$  run lengths.

than  $k$ . While recent work has considered information dynamics in 0-Markov brickwork circuits when unitaries drawn from a non-Haar distribution [16], these  $k$ -Markov circuits suggest a large class of related studies.

When the physical angle applied in each unitary is small (we use  $\theta = \pi/300$ ), short same-letter runs (lengths  $R$ ) move weight of about  $\sin^2[R\theta] \approx (R\theta)^2$  to operators with support on the neighboring qubit, generating a smooth light cone. Equilibration in terms of Hamming weight,  $w/N$ , is fastest, and smooth, when run lengths cluster at the longest length such that  $R\theta \lesssim 1$ . For examples shown before, we report  $t_w$ , the first compressed step where  $w/N \geq 0.50$ , for individual realizations and the average over many trials. When longer run-lengths can occur, the smooth spreading is punctuated by bursts that are large enough that  $R\theta$  is not small. As in the previous section, many different evolutions can give a comparable equilibration time to  $w/N$ , but the structure in the light cone and the correlation structure after equilibration will remain distinct. The quantity shown in the heatmaps is now the average occupation at site  $i$ ,  $d_i = \frac{1}{N} \sum_{\alpha: \mathcal{P}_{\alpha, i} \neq I} |c_{\alpha}|^2$ , where only operators that are not the identity at site  $i$  are included. Figure 3 shows several examples on 30 qubits, for which the equilibrium weight is empirically  $w/N \approx 0.52 - 0.53$ . The correlation panels are made with  $d_i$  in Eq.(1) (instead of  $n_i$ ).

Some properties of the gate sequence statistics can be understood by dividing the accessible Pauli strings into

two sectors:  $2N$  operators with only  $\sigma_z$  (and identity) operators, and  $N(2N - 2)$  'domain wall' strings where a single pair of  $\sigma_x, \sigma_y$  operators is separated by a string of  $\sigma_z$  operators. The initial operator is entirely in the  $Z$ -sector, and each PSWAP gate moves some weight into the domain wall sector. The weight in the domain wall sector is  $w_{\text{DW}} = \sum_{\alpha: n_{XY}(\mathcal{P}_{\alpha})=2} |c_{\alpha}|^2$ . The time-evolution of this weight, shown for several different models in Figure 4, shows how different run-length statistics, generated by different  $k$ -Markov models, act as filters for the frequencies visible in the weight evolution.

*Summary* - We have demonstrated that  $k$ -Markov sequences of unitary gates can be used to generate families of stochastic circuits that display a variety of structures in operator evolution. This very broad class of models has two components: the definition of an alphabet, constructed from some choice of unitary dynamics on a qubit network, and the specification of transition probabilities defining a  $k$ -Markov process on the alphabet. Within three choices of 2-letter alphabets, we demonstrated that many aspects of operator dynamics may be stochastically controlled, including transport dynamics, average spreading or equilibration times, relative weight in distinct symmetry sectors of the operator orbit, and structure in spatial-temporal correlations across the circuit that remain well after network-averaged equilibrium is achieved.

*Acknowledgments* - We thank Zhen Bi, Tommy Chin,

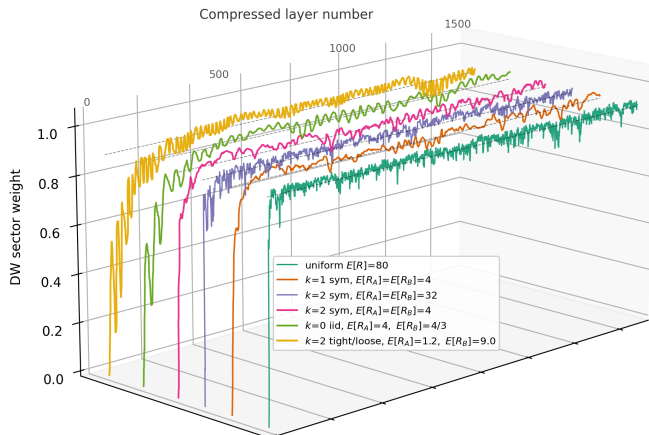


FIG. 4: The time evolution of the weight in the domain-wall sector of operators, for a single realization of each model scenarios shown in Figure 3 and two others. The  $k = 2$  symmetric case with  $E[R_A] = E[R_B] = 4$  shows that at small run length (and for the same seed), the difference between the geometric distributions at  $k = 1$  is small. The  $k = 2$  symmetric case with  $E[R_A] = E[R_B] = 32$  shows the different effective filter applied by distributions that contain more long run lengths.

Stefan Eccles, Jeysen Flores-Velazquez, Tom Iadecola, Dezhe Jin and Xiantao Li for helpful discussions. The work of Pei-Jun Huang was supported by the Penn State NSF REU through PHY-2349159. This work was supported by the NSF through PHY-2310662, and with computational resources supported by the NSF through OAC-2201445.

---

\* Corresponding author: ses47@psu.edu

- [1] A. Nahum, S. Vijay, and J. Haah, Operator spreading in random unitary circuits, *Phys. Rev. X* **8**, 021014 (2018).
- [2] V. Khemani, A. Vishwanath, and D. A. Huse, Operator spreading and the emergence of dissipative hydrodynamics under unitary evolution with conservation laws, *Phys. Rev. X* **8**, 031057 (2018).
- [3] Y. Li, X. Chen, and M. P. A. Fisher, Quantum zeno effect and the many-body entanglement transition, *Phys. Rev. B* **98**, 205136 (2018).
- [4] B. Skinner, J. Ruhman, and A. Nahum, Measurement-induced phase transitions in the dynamics of entanglement, *Phys. Rev. X* **9**, 031009 (2019).
- [5] A. Chan, R. M. Nandkishore, M. Pretko, and G. Smith, Unitary-projective entanglement dynamics, *Phys. Rev. B* **99**, 224307 (2019).
- [6] M. Knap, Entanglement production and information scrambling in a noisy spin system, *Phys. Rev. B* **98**, 184416 (2018).
- [7] T. Schuster and N. Y. Yao, Operator growth in open quantum systems, *Phys. Rev. Lett.* **131**, 160402 (2023).
- [8] Z. Weinstein, S. P. Kelly, J. Marino, and E. Altman, Scrambling transition in a radiative random unitary circuit, *Phys. Rev. Lett.* **131**, 220404 (2023).
- [9] Under a redefinition of the alphabet that enlarges the set of available unitaries,  $k$ -Markov circuits can be understood as  $k = 1$ , but they remain fundamentally distinct from  $k = 0$ .
- [10] R. Raussendorf and H. J. Briegel, A one-way quantum computer, *Phys. Rev. Lett.* **86**, 5188 (2001).
- [11] J. Zhang and S. L. Braunstein, Continuous-variable gaussian analog of cluster states, *Phys. Rev. A* **73**, 032318 (2006).
- [12] H. Buhрман, M. Folkertsma, B. Loff, and N. M. P. Neumann, State preparation by shallow circuits using feed forward, *Quantum* **8**, 1552 (2024).
- [13] L. Lovász and P. Winkler, A note on the last new vertex visited by a random walk, *Journal of Graph Theory* **17**, 593 (1993).
- [14] T. Gilbert and D. P. Sanders, Diffusion coefficients for multi-step persistent random walks on lattices, *Journal of Physics A: Mathematical and Theoretical* **43**, 035001 (2009).
- [15] N. Balakrishnan and M. V. Koutras, *Runs and Scans with Applications*, Wiley Series in Probability and Statistics (John Wiley & Sons, New York, 2002).
- [16] Z. Tan and P. W. Brouwer, Operator spreading in random unitary circuits with unitary-invariant gate distributions, *Phys. Rev. B* **111**, 184301 (2025).